Pergamon

Bioorganic & Medicinal Chemistry Letters 8 (1998) 641–646

BIOORGANIC & MEDICINAL CHEMISTRY LETTERS

MOLECULAR DYNAMICS SIMULATIONS OF THE STRUCTURE OF ALDOSE REDUCTASE COMPLEXED WITH THE INHIBITOR TOLRESTAT

Giulio Rastelli,* Luca Costantino

Dipartimento di Scienze Farmaceutiche, Via G. Campi 183, 41100 Modena, Italy.

Received 6 November 1997; accepted 6 February 1998

Abstract: This study reports a molecular dynamics (MD) investigation on the structure of aldose reductase (ALR2) complexed with the potent inhibitor tolrestat. The simulations predict four different orientations of tolrestat into the ALR2 binding site; these orientations have in common a strong interaction of the anionic carboxylate with Tyr48, His110, Trp111 and $NADP^+$, but completely differ for the orientation of the aromatic portion of the inhibitor. Interestingly, the orientation in which tolrestat gives the most attractive interaction energy with the enzyme is in full accord with the x-ray crystal structure of the complex that has been reported in the literature after this work was completed. In addition, the suggestion of more than one orientation of tolrestat during MD is in agreement with recent electrospray mass spectrometry experiments on the ALR2-tolrestat complex.

Aldose reductase (ALR2; EC1.1.1.21) is an enzyme of primary importance in the development of degenerative complications of diabetes mellitus, through its ability to reduce excess D-glucose into D-sorbitol.[1] Several aldose reductase inhibitors (ARIs) have been developed up to now.[2] Their structures mainly belong to the carboxylic acid and spirohydantoines classes of compounds, of which tolrestat and sorbinil are, respectively, two of the most important and studied members.

The crystallographic resolution of the structure of the enzyme, both isolated and complexed with the potent inhibitor zopolrestat, has revealed that ALR2 folds as a $(\beta/\alpha)_8$ barrel in which substrates and inhibitors bind at the bottom of a deep hydrophobic cleft.[3-6] Tyr48, His110 and Trp111 are three key residues in the recognition and hydrogen bonding of anionic inhibitors into the binding cleft. In addition, a strong electrostatic interaction between the positively charged $NADP^+$ and the anionic inhibitors occurs. The availability of x-ray structures of ALR2 prompted studies of structure-based drug design. We have recently docked and energy minimized a representative member of a new series of pyridazinone carboxylic acid compounds into the inhibitor binding site of ALR2.[7] More recently, we have performed a cycle of structure-based drug design that allowed us to design a new compound that proved to be a 100 fold better inhibitor than the starting inhibitor.[8]

In the present work, we extend our investigations on the ALR2-inhibitor interactions useful for drug design by reporting a theoretical analysis of the structure of the ALR2-tolrestat complex using molecular dynamics (MD).[9] Tolrestat is a highly flexible molecule compared to most other ARIs (Scheme 1); therefore it is challenging to use MD to investigate the conformational features of this molecule in relation to the possible binding orientations into ALR2.

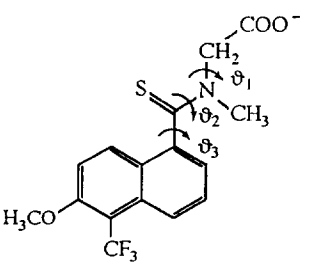

Scheme 1

e-mail giulio@unimo.it
fax +39-59-378560

0960-894X/98/$19.00
PII: S0960-894X(98)00083-3

A conformational analysis was performed on the isolated tolrestat molecule first. Figure 1 reports a monitoring of the ϑ_1, ϑ_2 and ϑ_3 dihedral angles (Scheme 1) during a 1000 ps MD simulation at 300°K. Three conformations have been obtained for tolrestat: conformation 1, which occurs during the 0-60ps and 340-460ps time intervals, has averaged angles of ϑ_1= 97°, ϑ_2=-157° and ϑ_3=46°; conformation 2 occurs between 60ps and 340ps, with averaged angles of ϑ_1=97°, ϑ_2=167° and ϑ_3=127°; finally, conformation 3 occurs during the last 460-1000ps, with averaged angles of ϑ_1=-110°, ϑ_2=167° and ϑ_3=128° . The most stable conformation is 3, followed by 2 (+1.3 kcal/mol) and 1 (+1.64 kcal/mol).

Figure 1: Monitoring of the ϑ_1, ϑ_2 and ϑ_3 dihedral angles of tolrestat during the 1000ps MD simulation

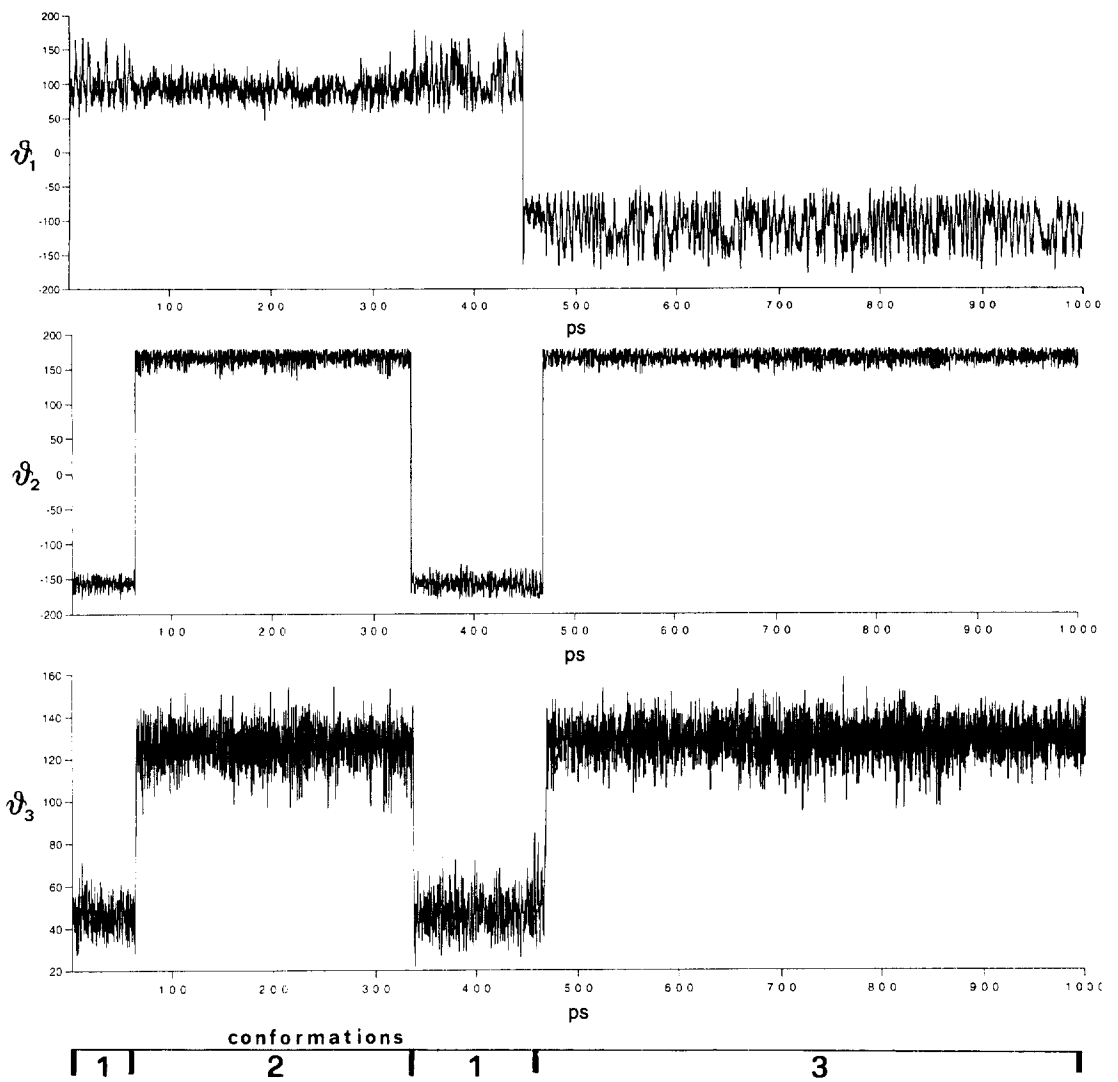

The three conformations of tolrestat revealed by MD were then considered for the docking of the inhibitor into the ALR2 binding site. Since the binding of inhibitors to ALR2 is known to cause severe conformational changes of loop 121-135 and segment 298-303 from both x-ray crystallography[6] and previous MD simulations,[7,8] two structures of ALR2 were initially used for this purpose: the first is the x-ray crystal structure of the holoenzyme,[4] and the second is the structure of ALR2 that we obtained after docking and energy-minimization of a bulky inhibitor into the binding site.[8] As already discussed, these two ALR2 structures differ mainly for an additional hydrophobic pocket lined by Trp111 and Leu300 in the inhibitor-bound form, which is closed in the holoenzyme.[8] While the anionic carboxylate of tolrestat must hydrogen bond Tyr48, His110 and Trp111 in both structures,[6-8] the hydrophobic portion of the inhibitor will be docked once outside (holoenzyme structure) and once inside (inhibitor-bound structure) the additional hydrophobic pocket, and the MD results will be compared.

Let's consider the docking of tolrestat into the structure of the holoenzyme first. Conformations 2 and 3 of tolrestat appear to be both suited to perform hydrogen bonds of the carboxylate with Tyr48, His110 and Trp111 without giving steric clash of the remaining bulky inhibitor with protein residues of the enzyme. Conformation 2 was docked into this structure and MD was started from the docked minimized complex and continued for over 500ps. As a result, conformation 2 holds for the first 100ps, after which a conformational change to 3 occurs. Figure 2(a) reports the monitoring of ϑ_1 (the torsional angle indicative of the conformational change 2 to 3) during MD, and shows the conformational change from an averaged angle of 82° to -130°. Coordinates of the complex were averaged at regular intervals for visual inspection. Interestingly, the change from conformation 2 to 3 in this enzyme simulation is indicative of two different binding orientations of tolrestat (orientations 1 and 2 in Figure 2a): the carboxylate hydrogen bonds Tyr48, His110 and Trp111 in both conformations, but the hydrophobic portion of the inhibitor interacts with different protein residues, as reported in Table 1.

Figure 2: Monitoring of the ϑ_1 dihedral angle during the 500ps MD simulations of tolrestat complexed with ALR2; simulations with tolrestat outside (a) and inside (b) the Trp111-Leu300 pocket

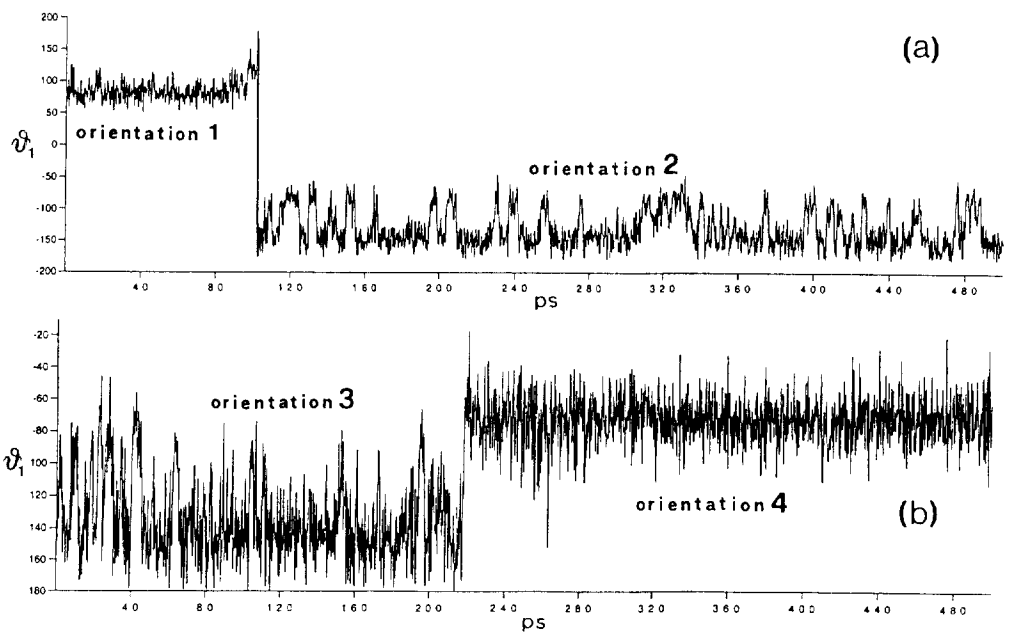

The second series of MD calculations were performed starting from the structure of the Trp111-Leu300 open form of ALR2. Conformation 3 of tolrestat was the most suited for interaction of the carboxylate with the usual hydrogen bonding residues and, at the same time, insertion of the bulky portion of the inhibitor into the open hydrophobic pocket of the enzyme. Since zopolrestat[6] and a pyridazinone inhibitor that we previously modeled[8] enter this cavity with complete stacking of a benzothiazole with Trp111, the same initial condition was tried with the aromatic ring of tolrestat by imposing some manual adjustment to conformation. Then, the complex was energy minimized and MD was run for 500ps. Again, the monitoring of ϑ_1, ϑ_2 and ϑ_3 angles was performed. The analysis of these MD simulations reveals that conformation 3 holds for the first 220ps, after which ϑ_1 turns to an average angle of -72° (Figure 2(b)). ϑ_2 and ϑ_3 are still characteristics of conformation 3. This last value for ϑ_1 was not observed in the isolated tolrestat, and must therefore be induced by ALR2. Indeed, coordinates averaged during MD show that this conformational change is concomitant with a change of orientation of tolrestat (orientations 3 and 4 in Figure 2b) inside ALR2.

Table 1 reports the residues interacting with the aromatic ring of tolrestat in the four orientations found by MD, together with the relative energy of each conformer of tolrestat and its interaction energy with ALR2. It is interesting to observe that orientations 3 and 4 show more attractive interaction energies with ALR2 (-57.8 and -61.2 kcal/mol, respectively) compared to orientations 1 and 2 (-52.4 and -51.3 kcal/mol, respectively). Therefore, the insertion of tolrestat into the Trp111-Leu300 additional pocket provide stronger interactions of the inhibitor with ALR2 at no expense (orientation 3) or at a very little expense (0.8 kcal/mol, orientation 4) of conformational energy.

Table 1: Protein residues in contact (3Å) with the aromatic ring of tolrestat, relative energies (kcal/mol) of each conformer (ΔE_{conf}) and interaction energies (ΔE_{int}) of the inhibitor with ALR2 in the four orientations found by MD.

Orientation 1:	Trp20, Phe122, Trp219, Cys298, Leu300, Leu301	ΔE_{conf}= 1.4	ΔE_{int}= -52.4
Orientation 2:	Trp20, Val47, Phe121, Phe122, Trp219, Leu300	ΔE_{conf}= 0	ΔE_{int}= -51.3
Orientation 3:	Trp20, Trp79, Trp111, Phe115, Phe122, Pro218, Trp219, Leu300	ΔE_{conf}= 0	ΔE_{int}= -57.8
Orientation 4:	Trp79, Trp111, Thr113, Phe115, Phe122, Val130, Ser302, Cys303	ΔE_{conf}= 0.8	ΔE_{int}= -61.2

In conclusion, our MD simulations of the ALR2-tolrestat complex reveal that tolrestat binds ALR2 in four different orientations. All orientations share the strong electrostatic interactions between the carboxylate and the positive nicotinamide ring and the hydrogen bonding to Tyr48, His110 and Trp111. However, they completely differ for the orientation of the hydrophobic portion of the inhibitor within the binding site, as inferred from the data in Table 1 and as graphically shown in Figure 3, where the four orientations of tolrestat and the nearby protein residues have been superimposed for comparison. Orientations 1 and 2 have the hydrophobic rings of tolrestat outside the additional hydrophobic pocket; orientations 3 and 4 have the hydrophobic rings of tolrestat inside this pocket, albeit in rather different orientations.

Figure 3: Stereoview of the superimposition of the four orientations of tolrestat (green=orientation 1, cyan=orientation2, yellow=orientation3, red=orientation4) into ALR2 found by MD, and nearby protein residues.

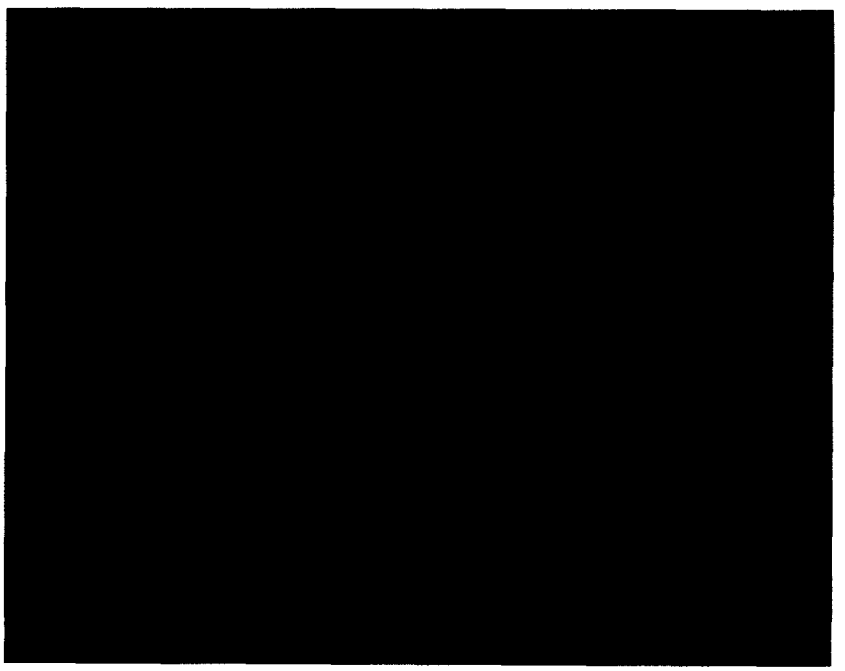

After this work was completed, the crystal structure of ALR2 complexed with tolrestat at 2.0Å resolution was reported.[10] It is significant that orientation 4, which is indeed the orientation in which tolrestat shows the most attractive interaction energy with ALR2, is in all identical to that observed by crystallography. Intriguingly, orientation 4 predicts that tolrestat binds in a position perpendicular to that occupied by zopolrestat in the ALR2-zopolrestat complex,[6] in full accord with the x-ray structure. This finding is particularly important in light of the conformational freedom of tolrestat and of the fact that the binding orientation of tolrestat had unprecedents in other ALR2-inhibitor crystal structures and molecular modelling calculations at the time this study was undertaken.

Finally, it is worth of mention that our MD simulations provide insight into the dynamics of the interaction of tolrestat with ALR2. Besides orientation 4, which coincides with the one observed by x-ray crystallography, the present MD simulations predict three more orientations of tolrestat into ALR2. In this regard, our simulations agree with recent electrospray mass spectroscopy experiments on the ALR2-tolrestat complex,[11] in which the presence of more than one fragmentation peak was attributed to the ability of tolrestat to give interactions with different binding environments within ALR2.

Acknowledgements

Financial support from CNR (grant n° 95.00954.CT03) and computer facilities from the Centro Interdipartimentale di Calcolo Elettronico (CICAIA) are gratefully acknowledged.

References

1. Tomlinson, D.R.; Stevens, E.J.; Diemel, L. *Trends Pharm. Sci.* **1994**, 15, 293-297.
2. Costantino, L.; Rastelli, G.; Cignarella, G.; Vianello, P.; Barlocco, D. *Exp. Opin. Ther. Patents* **1997**, 7, 1-16.
3. Rondeau, J.M.; Tete-Favier, F.; Podjarni, A. *Nature* **1992**, 355, 469-472.
4. Borhani, D.W.; Harper, T.M.; Petrash, J.M. *J. Biol. Chem.* **1992**, 267, 24841-24847 .
5. Wilson, D.K.; Bohren, K.M.; Gabbay, K.H.; Quiocho, F.A. *Science* **1992**, 257, 81-84.
6. Wilson, D.K.; Tarle, I.; Petrash, J.M.; Quiocho, F.A. *Proc. Natl. Acad. Sci. USA* **1993**, 90, 9847-9851.
7. Costantino, L.; Rastelli, G.; Vescovini, K.; Cignarella, G.; Vianello, P.; Del Corso, A.; Cappiello, M.; Mura, U.; Barlocco, D. *J. Med. Chem.* **1996**, 39, 4396-4405.
8. Rastelli, G.; Vianello, P.; Barlocco, D.; Costantino, L.; Dal Corso, A.; Mura, U. *Bioorg. Med. Chem. Lett.* **1997**, 7, 1897-1902.
9. Molecular dynamics (MD) simulations were performed using the AMBER4.1 program with the Cornell *et al.* force field on a SGI Power Challenge computer. Graphic display was performed with MIDAS.
   The two ALR2 structures used for MD are the crystal structure of the ALR2-NADP$^+$ holoenzyme (ref 4) and the ALR2 structure that we previously obtained after docking and energy-minimization of a bulky inhibitor in the active site (ref. 8). The geometry of tolrestat was completely optimized using the AM1 Hamiltonian. Parameters for tolrestat were set consistently to the Cornell *et al.* force field: missing bond and angle parameters were assigned on the basis of analogy with known parameters in the database, and calibrated to reproduce the AM1 optimized geometry. The partial charges on tolrestat were calculated from an electrostatic potential fit to a 6-31G* *ab-initio* wave function using Gaussian94, followed by RESP analysis.
   Tolrestat was docked into the ALR2 binding site as described in the text. 2000 steps of energy minimization were performed prior to MD for both the isolated tolrestat and the ALR2 complexes. All the protein residues within 12Å of each atom of the inhibitor were allowed to move. A distance-dependent dielectric constant with a 4r dependence, and a 10Å non-bonded cutoff were adopted in all simulations.
   MD calculations were performed at 300°K for 1000ps in the isolated tolrestat simulation, and for 500ps in the two ALR2-tolrestat simulations. SHAKE was turned on during MD. Coordinates were collected every 0.2ps. Coordinates averaging and dihedral angles monitoring during MD were performed using CARNAL. Other details can be found in ref.4.
10. Urzhumtsev, A.; Tete-Favier, F.; Mitschler, A.; Barbanton, J.; Barth, P.; Urzhumtseva, L.; Biellmann, J.F.; Podjarni, A.D.; Moras, D. *Structure* **1997**, 5, 601-612.
11. Potier, N.; Barth, P.; Tritsch, D.; Biellmann, J.F.; Van Dorsselaer, A. *Eur. J. Biochem.* **1997**, 243, 274-282.